12th International Kimberlite Conference Extended Abstract No. 12IKC-142, 2024

An experimental study on the kimberlitic magma evolution during ascent before emplacement

Zairong Liu[1], I-Ming Chou[1]

[1]*Institute of Deep-sea Science and Engineering (IDSSE), CAS, China, liuzr@idsse.ac.cn, imchou@idsse.ac.cn*

Introduction

Kimberlites are broadly seen as being generated in a CO_2-rich or carbonated mantle source or evolved from carbonatitic magmas (Dalton and Presnall, 1998; Le Roex et al., 2003; Wyllie, 1980); and references therein). As the proceeding of crystallization and dissolution of volatile in melts, the oxygen fugacity (fO_2) of kimberlitic melts increases progressively (Canil and Bellis, 2007; Casetta et al., 2023), regardless of the redox state of their mantle source. Although the oxygen fugacity of kimberlite source cannot be revealed directly, the effect of redox variation would be evidenced by the changes of mineral stabilities during kimberlitic magma fractionation. However, the temperature and oxygen fugacity conditions for the crystallization in the late stage of kimberlite melts evolution and the sequence crystallization are still poorly constrained (Giuliani et al., 2023), therefore, experiments are required to establish and verify these conditions. Given that kimberlitic melts are susceptible to serpentinization and crustal contamination at low pressure and temperature (Afanasyev et al., 2014), we conducted high-pressure and high-temperature experiments to simulate kimberlite magma evolution after rising from the source mantle before emplacement at the bottom of crust. The primary melt composition of kimberlite used in this study is based on that reconstructed from Group I aphanitic kimberlites from South Africa after correction of contaminated macrocryst (Becker and Roex, 2006; Sokol and Kruk, 2015). The starting material used in this study has been altered to contain slightly higher H_2O and CO_2, and could be regarded as more approximate to the primary kimberlite magma, considering the CO_2 degassing during kimberlite magma ascent and the extraction of H_2O from later serpentinization (Edgar et al., 1988).

Methods

We conducted high pressure experiments in a piston cylinder apparatus at 2-3 GPa, and temperatures between 900 and 1200 °C. We used two fO_2 settings (Fig. 1) with the double capsule technique (Eugster and Skippen, 1967) to buffer the required redox conditions. The first set was graphite-saturated C-COH fluid conditions (abbr. CCOH buffer, Ulmer and Luth, 1991), and the second set was Ni-NiO conditions (abbr. NNO buffer). All experiments were performed for 6-24 hours to ensure reaching chemical equilibrium. After experiments, the mineral and melts compositions were determined by scanning electron microscope (Apreo 2 SEM) at IDSSE and electron microprobe JOEL 8230 in the commercial analysis companies. The run conditions and results are reported in Table 1.

Results and discussion

Our results show that, magnesian ilmenite composition obtained in this study is characterised by 14.4-17.9 wt.% of MgO, comparable to the groundmass composition obtained in the hypabyssal kimberlite (Mitchell, 1977; Arculus et al., 1984). The clinopyroxene under both redox conditions is diopside, as to the case of micaceous hypabyssal kimberlite (Mitchell, 1986). Orthopyroxene was absent under all NNO buffered conditions, however, contrary to what is commonly believed that it is rare or absent in most kimberlites,

we observed orthopyroxene crystallization under CCOH buffered conditions at 2-3 GPa. Further, olivines in this study are rich in MgO (Fo_{83-95}) under both redox conditions, which are different from either megacrysts or microphenocrystal olivines in kimberlite rocks, but comparable to the xenocrystal olivines found in kimberlites (Mitchell, 1986, Giuliani et al., 2018). Although MgO-rich phenocrystic olivine are commonly absent or rare in kimberlite rocks, our studies indicates that olives formed from kimberlite fractional crystallization are MgO-rich and able to coexistent with the CO_2-rich fractionated melt.

Table 1: Experimental run conditions and phases assemblages in the experiments

Exp No.	P/GPa	T/°C	t/hr	Outer-inner	Buffer	Phases
KMB-2	3	1200	6	Pt-C	CCOH	Ol + Cpx + Opx + Phl* + Rt* + Melt
KMB0-3	3	1100	12	Pt-C	CCOH	Ol + Cpx + Opx +Mg-Ilm* + Rt + Phl + Melt
KMB-3	3	1000	24	Pt-C	CCOH	Ol + Cpx + Opx + Rt + Phl + Dol + Melt
KMB-7	3	1000	24	Au-Pt	NNO	Ol + Cpx + Mg-Ilm + Phl + Apt + Dol + Mgs
KMB-19	2.4	1200	7	Pt-C	CCOH	Ol + Opx + Phl* + Melt
KMB-18	2.4	1200	7	Au-Pt	NNO	Ol + Melt
KMB-26	2.4	1100	12	Pt-C	CCOH	Ol + Cpx + Melt
KMB-25	2.4	1100	12	Au-Pt	NNO	Ol + Melt
KMB-29	2.4	1000	24	Pt-C	CCOH	Ol + Cpx Mg-Ilm + Rt + Phl + Melt
KMB-22	2.4	1000	24	Au-Pt	NNO	Ol + Cpx + Rt + Phl + Melt
KMB-20	2	1200	7	Pt-C	CCOH	Ol + Melt
KMB-23#	2	1200	7	Pt-AuPd	NNO	Ol + Melt
KMB-27	2	1100	12	Pt-C	CCOH	Ol + Cpx + Melt
KMB-35	2	1100	12	Pt-AuPd	NNO	Ol + Cpx + Mg-Ilm + Phl + Melt
KMB-15	2	1050	12	Au-Pt	NNO	Ol + Cpx + Melt
KMB-21	2	1000	24	Pt-C	CCOH	Ol + Cpx + Mg-Ilm + Rt + Phl +Melt
KMB-11	2	1000	24	Au-Pt	NNO	Ol + Cpx + Mg-Ilm + Rt + Phl + Apt + Dol
KMB-14	2	950	12	Au-Pt	NNO	Ol + Cpx + Mg-Ilm + Phl + Apt + Dol
KMB-13	2	900	8	Au-Pt	NNO	Ol + Cpx + Mg-Ilm + Phl* + Apt + Dol

P-pressure, T-temperature, t-run duration in hour(s), Outer-inner-the material of outer and inner capsule, respectively, buffer-mineral oxygen fugacity buffer. Ol-olivine, Cpx-clinopyroxene, Opx-orthopyroxene, Rt-rutile, Phl-phlogopite, Mg-Ilm-magnesian ilmenite, Apt-apatite, Dol-dolomite, Mgs-magnesite. Mg-Ilm*: The grains were too small to be detected with EMPA and were only confirmed with SEM. KMB-23#: Inner capsule leaked.

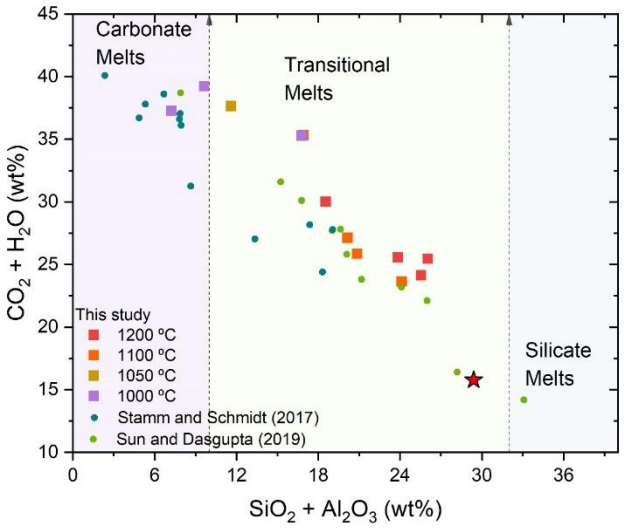

Figure 1: The residual compositions of kimberlite magma and comparison with those in previous studies. The red star represents the composition of the starting material used in this study.

As demonstrated by Fig. 1, the residual melt of kimberlite, derived from factional crystallization of kimberlite, features low SiO_2 + Al_2O_3 but high CO_2 + H_2O, and evolves to carbonatitic melts as the temperature decreases. Thus, the residual melt compositions obtained in this study are transitional between those of carbonate melts and silicate melts, supporting that kimberlite may fractionate to carbonatites (Stamm and Schmidt, 2017).

References

Afanasyev AA, Melnik O, Porritt L, et al (2014) Hydrothermal alteration of kimberlite by convective flows of external water. Contributions to Mineralogy and Petrology 168:1–17

Arculus RJ, Dawson JB, Mitchell RH, et al (1984) Oxidation states of the upper mantle recorded by megacryst ilmenite in kimberlite and type A and B spinel lherzolites. Contributions to Mineralogy and Petrology 85:85–94

Becker M, Roex APL (2006) Geochemistry of South African on-and off-craton, Group I and Group II kimberlites: petrogenesis and source region evolution. Journal of Petrology 47:673–703.

Canil D, Bellis AJ (2007) Ferric Iron in $CaTiO_3$ Perovskite as an Oxygen Barometer for Kimberlite Magmas II: Applications. Journal of Petrology 48:231–252.

Casetta F, Asenbaum R, Ashchepkov I, et al (2023) Mantle-derived cargo vs liquid line of descent: reconstructing the P–T–fO_2–X Path of the Udachnaya–East kimberlite melts during ascent in the Siberian sub-cratonic lithosphere. Journal of Petrology 64:egac122.

Dalton JA, Presnall DC (1998) The continuum of primary carbonatitic–kimberlitic melt compositions in equilibrium with lherzolite: data from the system CaO–MgO–Al_2O_3–SiO_2–CO_2 at 6 GPa. Journal of Petrology 39:1953–1964

Edgar AD, Arima M, Baldwin DK, et al (1988) High-pressure-high-temperature melting experiments on a SiO2-poor aphanitic kimberlite from the Wesselton Mine, Kimberley, South Africa. American Mineralogist 73:524–533

Eugster HP, Skippen GB (1967) Igneous and metamorphic reactions involving gas equilibria. Wiley

Giuliani A (2018) Insights into kimberlite petrogenesis and mantle metasomatism from a review of the compositional zoning of olivine in kimberlites worldwide. Lithos 312–313:322–342

Giuliani A, Schmidt MW, Torsvik TH, Fedortchouk Y (2023) Genesis and evolution of kimberlites. Nature Reviews Earth & Environment 4:738–753

Le Roex AP, Bell DR, Davis P (2003) Petrogenesis of group I kimberlites from Kimberley, South Africa: evidence from bulk-rock geochemistry. Journal of Petrology 44:2261–2286

Mitchell RH (1977) Geochemistry of magnesian ilmenites from kimberlites in South Africa and Lesotho. Lithos 10:29–37

Mitchell RH (1986) Mineralogy of kimberlites. In: Kimberlites. Springer, pp 137–274

Safonov OG, Kamenetsky VS, Perchuk LL (2011) Links between Carbonatite and Kimberlite Melts in Chloride–Carbonate–Silicate Systems: Experiments and Application to Natural Assemblages. Journal of Petrology 52:1307–1331

Sokol AG, Kruk AN (2015) Conditions of kimberlite magma generation: experimental constraints. Russian Geology and Geophysics 56:245–259

Stamm N, Schmidt MW (2017) Asthenospheric kimberlites: volatile contents and bulk compositions at 7 GPa. Earth and Planetary Science Letters 474:309–321

Sun C, Dasgupta R (2019) Slab–mantle interaction, carbon transport, and kimberlite generation in the deep upper mantle. Earth and Planetary Science Letters 506:38–52

Ulmer P, Luth RW (1991) The graphite-COH fluid equilibrium in P, T, fO_2 space. Contributions to Mineralogy and Petrology 106:265–272

Wyllie PJ (1980) The origin of kimberlite. Journal of Geophysical Research: Solid Earth 85:6902–6910